



Get Clarity On Generics

Cost-Effective CT & MRI Contrast Agents



**FRESENIUS
KABI**

WATCH VIDEO

AJNR

Quantitative Susceptibility Mapping of Venous Vessels in Neonates with Perinatal Asphyxia

A.M. Weber, Y. Zhang, C. Kames and A. Rauscher

AJNR Am J Neuroradiol published online 1 April 2021
<http://www.ajnr.org/content/early/2021/04/01/ajnr.A7086>

This information is current as of August 6, 2025.

Quantitative Susceptibility Mapping of Venous Vessels in Neonates with Perinatal Asphyxia

A.M. Weber, Y. Zhang, C. Kames, and A. Rauscher



ABSTRACT

BACKGROUND AND PURPOSE: Cerebral venous oxygen saturation can be used as an indirect measure of brain health, yet it often requires either an invasive procedure or a noninvasive technique with poor sensitivity. We aimed to test whether cerebral venous oxygen saturation could be measured using quantitative susceptibility mapping, an MR imaging technique, in 3 distinct groups: healthy term neonates, injured term neonates, and preterm neonates.

MATERIALS AND METHODS: We acquired multiecho gradient-echo MR imaging data in 16 neonates with perinatal asphyxia and moderate or severe hypoxic-ischemic encephalopathy (8 term age: average, 40.0 [SD, 0.8] weeks' gestational age; 8 preterm, 33.5 [SD, 2.0] weeks' gestational age) and in 8 healthy term-age controls (39.3 [SD, 0.6] weeks, for a total of $n = 24$). Data were postprocessed as quantitative susceptibility mapping images, and magnetic susceptibility was measured in cerebral veins by thresholding out 99.95% of lower magnetic susceptibility values.

RESULTS: The mean magnetic susceptibility value of the cerebral veins was found to be 0.36 (SD, 0.04) ppm in healthy term neonates, 0.36 (SD, 0.06) ppm in term injured neonates, and 0.29 (SD, 0.04) ppm in preterm injured neonates. Correspondingly, the derived cerebral venous oxygen saturation values were 73.6% (SD, 2.8%), 71.5% (SD, 7.4%), and 72.2% (SD, 5.9%). There was no statistically significant difference in cerebral venous oxygen saturation among the 3 groups ($P = .751$).

CONCLUSIONS: Quantitative susceptibility mapping–derived oxygen saturation values in preterm and term neonates agreed well with values in past literature. Cerebral venous oxygen saturation in preterm and term neonates with hypoxic-ischemic encephalopathy, however, was not found to be significantly different between neonates or healthy controls.

ABBREVIATIONS: χ = magnetic susceptibility; CSaO₂ = cerebral arterial oxygen saturation; CSvO₂ = cerebral venous oxygen saturation; Hct = hematocrit; HIE = hypoxic-ischemic encephalopathy; NIRS = near-infrared resonance spectroscopy; QSM = quantitative susceptibility mapping; SSS = superior sagittal sinus; TRUST = T2-relaxation-under-spin tagging

Perinatal asphyxia is the condition resulting from the deprivation of oxygen to a neonate and can lead to brain tissue damage or death. Asphyxia at birth can affect virtually any organ, but the brain is of the highest concern because it is the least likely to quickly or completely heal.¹ Hypoxic-ischemic encephalopathy (HIE) occurs when the entire brain is deprived of an adequate supply of oxygen and can result in neurologic disability, such as cerebral palsy, mental retardation, and epilepsy. HIE occurs in

1.5 per 1000 live births² and is the fifth leading cause of death worldwide in children younger than 5 years of age (8%).³

Currently, the severity of HIE is mainly assessed by clinical parameters and conventional MR imaging and can be classified into mild, moderate, or severe categories.^{4,5} While identifying HIE in term infants is generally well-characterized, its identification in preterm infants remains complex, with variable inclusion criteria being discussed and reported.⁶⁻⁹ More accurate markers would be useful

Received December 7, 2020; accepted after revision January 14, 2021.

From the Division of Neurology (A.M.W., A.R.), Department of Pediatrics and University of British Columbia MRI Research Centre (A.M.W., C.K., A.R.), Department of Physics and Astronomy (C.K., A.R.), and Department of Radiology (A.R.), University of British Columbia, Vancouver, British Columbia, Canada; Department of Radiology (Y.Z.), Children's Hospital of Chongqing Medical University, Chongqing, China; Ministry of Education Key Laboratory of Child Development and Disorders (Y.Z.), Chongqing, China; Key Laboratory of Pediatrics in Chongqing (Y.Z.), Chongqing, China; Chongqing International Science and Technology Cooperation Center for Child Development and Disorders (Y.Z.), Chongqing, China.

A.M. Weber and Y. Zhang contributed equally to this work.

A.M. Weber was supported by a British Columbia Children's Hospital Research Institute, M.I.N.D. postdoctoral fellowship. A. Rauscher is supported by Canada Research Chairs and a Natural Sciences and Engineering Council of Canada grant (402039-2011, RGPIN-2016-05371).

Please address correspondence to Alexander Mark Weber, PhD, BC Children's Hospital Research Institute, Variety Building, Room 370B, 950 West 28th Ave, Vancouver, BC, Canada V5Z 4H4; e-mail: alex.weber@ubc.ca; @AlexMarkWeber

Indicates open access to non-subscribers at www.ajnr.org

Indicates article with online supplemental data.

<http://dx.doi.org/10.3174/ajnr.A7086>

for detection, classification, early therapeutic interventions, and predictors of long-term outcome. Several studies have investigated various alternative methods for measuring HIE, such as DWI,¹⁰ MR spectroscopy,^{11,12} urinary nuclear MR metabolomic profiling,¹³ and visual evoked potentials,¹⁴ with varying levels of reported success.

Cerebral venous oxygen saturation (CSvO₂) is the amount of leftover oxygen in the veins after oxygen delivery and extraction by the brain and can act as a surrogate of brain oxygen consumption. The oxygen supply is of critical importance to brain function because neurons rely predominantly on aerobic metabolism for their energy demands. In infants who have experienced birth asphyxia, CBF has been reported to be markedly elevated.¹⁵ When the brain is hyperperfused like this, elevated CSvO₂ values would signal a “luxury perfusion” state, suggesting serious brain damage.¹⁶ Normal CSvO₂ values, meanwhile, would suggest intact coupling between CBF and metabolic needs.¹⁷ Thus, knowing the CSvO₂ in preterm and term infants who are suspected of having HIE could provide clinicians with invaluable information. Unfortunately, the 2 current methods for measuring CSvO₂ require either the invasive insertion of an internal jugular vein catheter for co-oximetry or a blood gas analyzer, or the noninvasive use of near-infrared resonance spectroscopy (NIRS). NIRS, however, has been shown to have poor sensitivity at low CSvO₂ compared with co-oximetry and can reach a depth of only a few millimeters.¹⁸

Quantitative susceptibility mapping (QSM)^{19,20} examines gradient-echo phase data, usually acquired with SWI,²¹ to determine local tissue magnetic susceptibility (χ). Because deoxyhemoglobin in the venous blood is paramagnetic, a decrease in χ of venous blood compared with the surrounding brain tissue will indicate increased CSvO₂. Thus, QSM, a noninvasive method, may provide an indirect measure of CSvO₂.^{22,23} For example, Doshi et al,²⁴ in 2015, reported increased CSvO₂ in adults following mild traumatic brain injury. Similarly, Chai et al,²⁵ in 2017, reported increased CSvO₂ in subjects with mild traumatic brain injury compared with healthy controls, but they also reported a positive correlation of CSvO₂ with postconcussive symptoms. Chai et al,²⁶ in 2020, also reported reduced CSvO₂ in patients undergoing hemodialysis, which also correlated with cognitive scores ($r = 0.492$, $P = .02$).

Thus, we set out to determine how well CSvO₂ could be measured using QSM and hematocrit (Hct) from blood samples in term and preterm neonates with moderate or severe HIE and to compare those values with those of healthy term controls. We hypothesized that after perinatal asphyxia, both preterm and term neonates with moderate or severe HIE would demonstrate increased CSvO₂ through decreased cerebral vein magnetic susceptibility compared with healthy term controls.

MATERIALS AND METHODS

Patients

Between January 2017 and January 2018, preterm and term neonates with a clinical history of perinatal asphyxia and moderate or severe HIE who were transferred to Children’s Hospital of Chongqing Medical University intensive care nursery were enrolled in a study evaluating the detection of brain injury by MR imaging, in accordance with The Code of Ethics of the World Medical Association (Declaration of Helsinki). Recruitment and

scanning ended due to the neonatal ward of the hospital moving to a new branch of the hospital, where their scanners were from a different vendor, and there were no Phillips Healthcare scanners. The institution’s Committee on Clinical Research Ethics approved the study protocol, and informed consent was obtained from the parents. The inclusion criteria were determined on the basis of the definition of perinatal asphyxia and moderate or severe HIE as follows: 1) evidence of perinatal asphyxia (Apgar score of ≤ 7 for > 5 minutes after birth or a history of acute perinatal event, placental abruption, cord prolapse, or the need for ventilation for at least 10 minutes after birth²⁷); 2) evidence of moderate or severe HIE distinguished by using the Sarnat and Sarnat clinical stages⁵ for term infants and infants between 33 and 37 weeks’ gestation and significant changes in neurologic examination findings and/or seizures for infants younger than 33 weeks gestation;²⁸ and 3) abnormal MR imaging findings in all patients on T1-weighted, T2-weighted, and FLAIR images, mainly but not only in the basal ganglia/thalami region, watershed region, and periventricular white matter caused by HIE.^{29,30} Subjects were sedated using 5 mg/kg of phenobarbital (intramuscular injection). Neonates with high motion or image artifacts were excluded. In total, 8 term neonates and 8 preterm neonates who were determined to have perinatal asphyxia and moderate or severe HIE were included for further study. Eight term neonates with hyperbilirubinemia who were free of other neonatal complications, such as congenital and chromosomal abnormalities and with normal MR imaging findings were recruited prospectively as healthy controls. Hct values were obtained as part of the regular clinical work-up.

MR Imaging Acquisition

Brain MR images were obtained on a 3T system (Achieva; Philips Healthcare) using an 8-channel sensitivity encoding head coil. Data for QSM were collected using a 3D gradient-echo sequence with 5 echoes (TR = 30 ms, TE1 = 4.5 ms, echo spacing = 5.5 ms, flip angle = 17°, FOV = $196 \times 154 \times 103 \text{ mm}^3$, acquired voxel size = $0.50 \times 0.5 \times 1.0 \text{ mm}^3$, reconstructed voxel size = $0.5 \times 0.5 \times 0.5 \text{ mm}^3$, scan time = 5 minutes 9 seconds).³¹ Other scans included the following: inversion recovery turbo spin-echo T1-weighted (TR/TI = 7000/600 ms, TE = 15 ms, section thickness = 5 mm, FOV = $160 \times 151 \times 98 \text{ mm}^3$, acquisition matrix = 220×163 , scan time = 2 minutes 17 seconds); turbo spin-echo T2-weighted (TR = 5000 ms, TE = 100 ms, section thickness = 5 mm, FOV = $160 \times 149 \times 98 \text{ mm}^3$, acquisition matrix = 332×205 , scan time = 1 minute 38 seconds); and fast FLAIR images (TR/TI = 12,000/2850 ms, TE = 140 ms, section thickness = 5 mm, FOV = $160 \times 149 \times 98 \text{ mm}^3$, acquisition matrix = 176×144 , scan time = 3 minutes 55 seconds). The total acquisition time was 13 minutes 23 seconds.

MR Imaging Analysis

QSM images of all 5 echoes were postprocessed from the phase data of the multi-gradient-echo scans. Phase unwrapping was achieved using a 3D Laplacian algorithm,³² while the background field was removed using the variable sophisticated harmonic artifact reduction for phase method.³³ A Gaussian filter ($\sigma = 0.5$) was applied to the normalized field maps to smooth out high-frequency errors originating from the reconstruction steps before

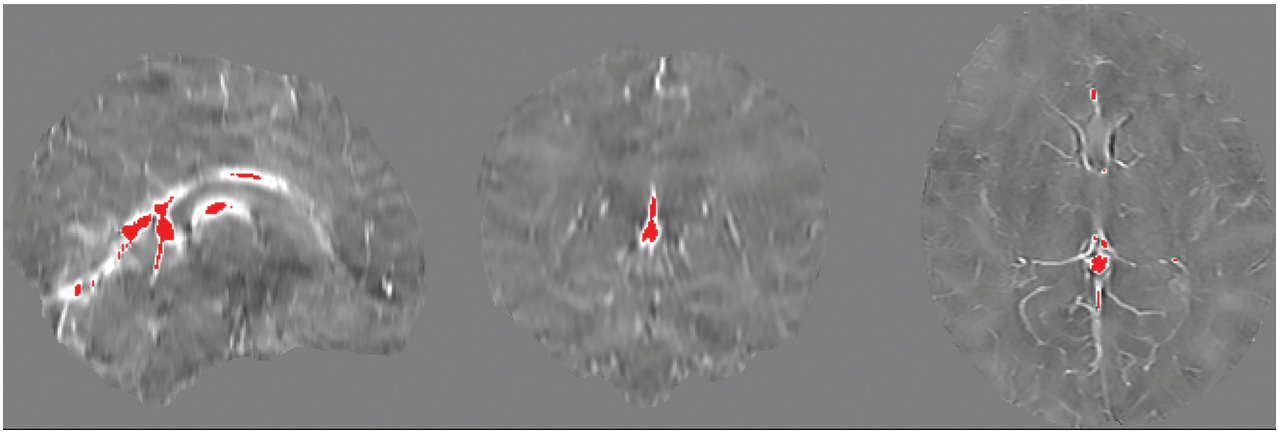


FIG 1. Sample internal veins selected after thresholding out the lower 99.95% χ values. As can be seen in these sagittal, coronal, and axial views from a sample healthy term neonate, the major veins that were left over include the straight sinus, inferior sagittal sinus, and the internal cerebral vein. Note the weak contrast between gray and white matter and the basal ganglia due to the low myelin and iron content of the neonate brain.

the inversion. A 2-step dipole inversion algorithm³⁴ was used to solve the dipole inversion problem. The last echo was used to obtain the brain mask, which effectively removed the external cerebral veins. Using the last echo to generate the brain mask reliably removed artifacts from air-tissue and bone-tissue interfaces, eg, sinuses, especially in the later echoes, without the need for manual erosion. This QSM algorithm can be freely accessed at <https://github.com/kamesy/QSM.m>. Finally, only the fourth echo (TE = 21 ms) was used for measuring χ values because even echoes were flow-compensated along the readout direction and the second echo (TE = 10 ms) had a poor contrast-to-noise ratio.

The χ of cerebral veins was measured by thresholding out the lowest 99.95% values of the whole brain. In the absence of intracranial hemorrhage and because neonates have very low brain iron content, voxels that reside entirely inside veins reflect the structures with the highest magnetic susceptibility values. Total blood volume is about 3%.^{35,36} Venous blood volume is about two-thirds of total blood volume. For a voxel to be free of partial volume effects and given the spatial resolution of $0.5 \times 0.5 \times 1 \text{ mm}^3$ of the scan, only veins with an inner diameter of at least 1 mm could be included in the analysis. After thresholding, images were assessed by A.M.W. to ensure that only veins remained (Fig 1). The remaining 0.25% of χ values was then averaged to give the mean cerebral χ value for each subject. ROIs were also drawn manually on nonvein tissue by A.M.W. to calculate $\Delta\chi$. Visual inspection did not reveal any germinal matrix bleeding in the deep cerebral veins.

Calculating CSvO₂

CSvO₂ was calculated using the following equation:

$$\Delta\chi = \Delta\chi_{do} \times HCT \times (1 - CSvO_2),$$

where $\Delta\chi$ is the susceptibility difference between venous blood and surrounding tissue, $\Delta\chi_{do}$ is the susceptibility difference per unit hematocrit between fully deoxygenated and fully oxygenated blood, Hct is the individual fractional hematocrit, and CSvO₂ is the blood oxygen saturation. $\Delta\chi_{do}$ was taken to be $4 \times \pi \times 0.21$, or 2.64 ppm.^{37,38}

Statistical Analysis

Statistical analysis was performed using R 3.4.2 (2017; <http://www.r-project.org/>). The relationship between calculated CSvO₂ and condition (healthy control, preterm injury, and term injury) was investigated using a 1-way ANOVA. Visual inspection of residual plots did not reveal any obvious deviations from homoscedasticity or normality.

RESULTS

Patient Characteristics

Demographic data and clinical characteristics for both groups (8 healthy controls, 8 term neonates, and 8 preterm neonates with perinatal asphyxia and moderate or severe HIE) are summarized in Table 1. No significant differences were found in gestational age, corrected gestational age at MR imaging, time interval between age at birth and age at MR imaging, birth weight, or sex between healthy controls and term neonates with HIE. No significant differences were found in sex, time interval between age at birth and age at MR imaging, clinical history, and symptoms and signs between term neonates and preterm neonates with perinatal asphyxia and moderate or severe HIE. As expected, a significant difference ($P < .05$) was found in the Apgar grade between healthy term neonates and term neonates with HIE. Between term and preterm neonates with HIE, significant differences ($P < .05$) were found only in gestational age, corrected gestational age at MR imaging, and birth weight, as would be expected.

CSvO₂ Analysis

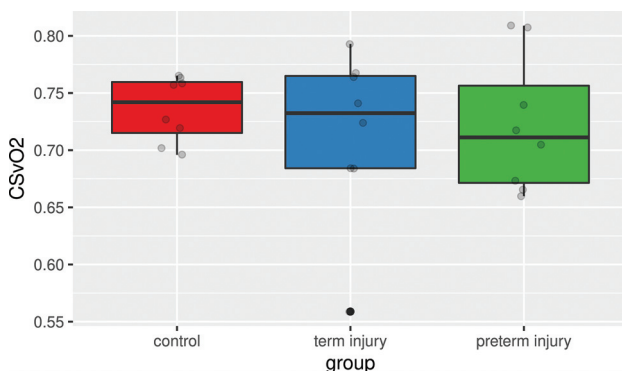
The mean χ value of the internal cerebral veins in healthy controls and term and preterm injured neonates was found to be 0.36 (SD, 0.04) ppm, 0.36 (SD, 0.06) ppm, and 0.29 (SD, 0.04) ppm, respectively, while the mean fractional Hct values were 0.52 (SD, 0.03), 0.49 (SD, 0.07), and 0.42 (SD, 0.06), respectively. Correspondingly, the derived mean CSvO₂ values were 73.6% (SD, 2.8%), 71.5% (SD, 7.4%), and 72.2% (SD, 6.0%), respectively. The Cohen D effect size between each group was found to be 0.38 for healthy controls and term injured neonates; 0.30 for healthy controls and preterm neonates; and 0.10 between term injured neonates and preterm

Table 1: Demographic data and clinical characteristics of the 3 groups^a

Characteristics	Healthy Controls (n = 8)	Term Neonates with HIE (n = 8)	P Value between Controls and Term HIE	Preterm Neonates with HIE (n = 8)	P Value between Term and Preterm HIE
Gestational age (mean) (wk)	39.3 (SD, 0.6)	40.0 (SD, 0.8)	.056	33.5 (SD, 2.1)	<.001
Corrected gestational age at MRI (mean) (wk)	41.3 (SD, 1.1)	41.9 (SD, 0.7)	.166	35.7 (SD, 2.6)	<.001
Time interval between age at birth and age at MR imaging (mean) (wk)	2.0 (SD, 0.7)	1.9 (SD, 0.6)	.819	2.2 (SD, 0.9)	.404
Birth weight (mean) (g)	3306.3 (SD, 353.1)	3430.6 (SD, 471.4)	.560	1926.3 (SD, 350.3)	<.001
No. of male neonates (No.) (%)	4 (50)	5 (62.5)	1.000	4 (50)	1.000
Apgar grade (median) (IQR)	10 (10–10)	6.5 (4–7)	<.001	6 (2–7)	.543
Umbilical cord around the neck (No.) (%)	2 (25)	1 (12.5)	1.000	1 (12.5)	1.000
Oxygen inhalation (No.) (%)	0	4 (50)	NA	7 (87.5)	1.000
Pulse oximetry (%)	95–100	90–95	<.001	90–95	.122
Meconium-stained amniotic fluid (No.) (%)	0	3 (37.5)	NA	1 (12.5)	.569
Premature rupture of fetal membranes (No.) (%)	0	3 (37.5)	NA	5 (62.5)	.619
Placental abruption (No.) (%)	0	0	NA	2 (25)	NA
Cord prolapse (No.) (%)	0	0	NA	1 (12.5)	NA
Fetal intrauterine distress (No.) (%)	0	7 (87.5)	NA	2 (25)	.119
Neonatal asphyxia resuscitation (No.) (%)	0	8 (100)	NA	8 (100)	NA
Respiratory failure and ventilation (No.) (%)	0	2 (25)	NA	5 (62.5)	.315
Obtundation (No.) (%)	0	7 (87.5)	NA	6 (75)	1.000
Stuporous (No.) (%)	0	1 (12.5)	NA	2 (25)	1.000
Inhibited primitive reflexes (No.) (%)	0	7 (87.5)	NA	6 (75)	1.000
Disappeared primitive reflexes (No.) (%)	0	1 (12.5)	NA	2 (25)	1.000
Hypotonia (No.) (%)	0	2 (25)	NA	4 (50)	.608
Flaccid (No.) (%)	0	1 (12.5)	NA	2 (25)	1.000
Seizures (No.) (%)	0	2 (25)	NA	3 (37.5)	1.000
Therapeutic hypothermia (No.) (%)	0	2 (25)	NA	1 (12.5)	1.000

Note:—IQR indicates interquartile range; NA, not applicable.

^a P values were from the χ^2 test or Fisher exact test for categorical variables or the Student t test for continuous variables.

**FIG 2.** Boxplot of CSvO₂ percentages by group. Gray circles are the ROI measurements from each subject.

neonates. A CSvO₂ boxplot among the 3 groups with individual points for each subject is shown in Fig 2. One-way ANOVA analysis did not reveal that the condition (healthy control, preterm injury, and term injury) made a significant difference among groups ($P > .05$). Boxplots of χ and Hct values in each group, with individual points for each subject are included in the Online Supplementary Data.

DISCUSSION

In this study, we quantified CSvO₂ from χ values in the internal cerebral veins of preterm and term neonates with HIE and healthy term controls. Moderate-to-severe HIE caused by intrapartum or late antepartum hypoxic-ischemic events may lead to neurodevelopmental disability.¹ It is of great importance to examine cerebral hemodynamic changes in neonates with moderate or severe HIE because this examination may lead to a better understanding of the cerebral oxygen metabolism of brain injury in HIE and early therapeutic interventions. Although no statistical difference in CSvO₂ values was found between healthy term controls and preterm and term infants with moderate or severe HIE, to the best of our knowledge, this is one of the first studies measuring CSvO₂ using QSM in healthy term neonates, as well as the first to do so in term and preterm neonates with moderate or severe HIE. Thus, our reported values for healthy neonates as well as injured preterm and term neonates may be used in future studies for comparison purposes. These values agree well with previously reported values using other methods (Table 2).

Noninvasive measurements of CSvO₂ in neonates has historically been quite difficult. The current best practice, NIRS, does not provide robust and reliable measurements due to several limitations,^{39,40} including contamination from extracerebral tissue

Table 2: Comparison of CSvO₂ percentages in fetuses and neonates in the literature

Study	CSvO ₂ (mean) (%)	Method	Subjects	Region
van der Hoeven et al ⁵⁷	73.56 (SD, 5.25)	Fiber optic catheter	Healthy neonates	
Buchvald et al ⁵⁸	64.12 (SD, 4.6)	NIRS	Healthy neonates	Frontotemporal region
Wintermark et al ⁵⁹	77.3 (SD, 4.7)	NIRS	Hypothermia therapy (moderate) in neonatal HIE	Frontal lobe
Wintermark et al ⁵⁹	77.6 (SD, 6.6)	NIRS	Hypothermia therapy (severe) in neonatal HIE	Frontal lobe
De Vis et al ⁶⁰	65.0 (SD, 13.0)	T2-TRIR	Healthy neonates	SSS
Shetty et al ⁴⁸	73.2 (SD, 5.5)	TRUST	Hypothermia therapy in neonatal HIE	SSS
Shetty et al ⁴⁸	68.5 (SD, 9.6)	TRUST	Post-hypothermia therapy in neonatal HIE	SSS
Liu et al ⁴⁹	62.6 (SD, 8.3)	TRUST	Healthy neonates	SSS
Yadav et al ⁴⁴	67 (SD, 7)	QSM	Healthy fetuses (~31 wk)	SSS
Jain et al ⁴⁵	55.2	Susceptometry	Neonates with congenital heart disease	SSS
Yadav et al ⁴⁶	62.6 (SD, 3.25)	Susceptometry	Healthy fetuses (~31 wk)	SSS
Neelavalli et al ⁴⁷	66 (SD, 9.4)	Susceptometry	Healthy fetuses (~34 wk)	SSS
Average	68.12			

Note:—T2-TRIR indicates T2-prepared tissue relaxation inversion recovery; SSS, superior sagittal sinus; TRUST, T2-relaxation-under-spin tagging; QSM, quantitative susceptibility mapping; NIRS, near infrared resonance spectroscopy.

and arterial blood (generally 30% but can vary considerably among subjects)⁴¹ and an insensitivity to low CSvO₂ levels.¹⁸ QSM, meanwhile, is a relatively new technique, which fully quantifies χ using MR imaging phase data. Because oxyhemoglobin is diamagnetic and deoxyhemoglobin is paramagnetic, a reduction in deoxyhemoglobin and an increase in oxyhemoglobin will be reflected as a decrease in the χ of venous blood. Using Hct values obtained from blood samples, one can then calculate the CSvO₂.

Recently, several studies have been published demonstrating the promise^{22,42,43} of using QSM to quantify CSvO₂ changes in brain injuries of adults.^{24,25} Doshi et al²⁴ and Chai et al²⁵ reported CSvO₂ differences between adult healthy controls and subjects with mild traumatic brain injury by measuring the χ of cerebral major veins. Doshi et al found decreases in venous χ in the left thalamostriate vein and right basal vein, while Chai et al found decreases in venous χ in the straight sinus. Both of these studies suggested increased CSvO₂ after a mild traumatic brain injury, with different conclusions as to what this might suggest. Doshi et al also obtained CBF measurements and found injured subjects to have significantly increased CBF postinjury. Along with the increase in CSvO₂, they suggested that the brain responds to traumatic injuries by trying to protect brain tissue via the supply of more oxygen than the tissue requires. Whereas Chai et al did not acquire CBF measures but did look at the correlation of χ reductions with the amount of time post-trauma, they reported a positive correlation between the 2 measures, which indicates recovery to normal levels of oxygenation with time. Chai et al suggested that QSM can thus be used as a biomarker and to monitor progress.

Closer to our study, Yadav et al⁴⁴ used QSM to measure CSvO₂ in healthy fetuses ($n = 21$, median week of pregnancy = 31.3). They reported a mean CSvO₂ of 67% (SD, 7%) in the superior sagittal sinus (SSS) vein, an external cerebral vein that is less than our reported values in internal cerebral veins in healthy controls (73.6% [SD, 2.84%]). Similarly, several studies have used a method analogous to QSM, known as MR susceptometry, which uses a susceptibility-weighted image to measure χ values on the basis of geometric assumptions (such as the SSS vein being an infinitely long cylinder). These studies reported CSvO₂ values in the SSS ranging from 55.2% in neonates with congenital heart disease⁴⁵ to 66% in 34-week-old healthy fetuses (Table 2).^{46,47}

Along with the susceptibility-based methods of measuring CSvO₂ in neonates and fetuses, there have been other MR imaging-related techniques worth mentioning. One such method is known as T2-relaxation-under-spin tagging (TRUST). For instance, Shetty et al,⁴⁸ in 2019, reported CSvO₂ changes during and after therapeutic hypothermia in neonatal HIE using TRUST. The CSvO₂ was calculated by measuring $1/T_2$ (R_2) of the SSS. They examined CSvO₂ values during early hypothermia treatment (18–24 hours after initiating treatment) and after and found posttreatment CSvO₂ to have been reduced from 73.2% (SD, 5.5%) (during treatment) to 68.5% (SD, 9.6%) (posttreatment). These posttreatment values agreed well with a previous study that reported 62.6% (SD, 8.3%) in healthy infants using the same method.⁴⁹ While these initial reports of measuring CSvO₂ using TRUST are promising, some drawbacks should be considered. On the one hand, the measurement of R_2 is relatively easier to postprocess than QSM because it requires only a few simple steps. On the other hand, unlike QSM, the measurement of R_2 has confounding factors such as fat, fibrosis, and edema,⁵⁰ along with saturation and blooming artifacts. Additionally, the scan required for QSM provides a wealth of additional information such as R_2^* maps and SWI, which can be used to better characterize lesions.⁵¹ In fact, SWI is already often used in clinical settings to detect intracranial hemorrhages and other brain abnormalities and is often part of the neonatal and pediatric MR imaging protocols.^{52–54} The scan is fast (<3 minutes on modern scanners) even at high spatial resolution (<1 mm³). Disadvantages in QSM include a range of different approaches for background field removal, dipole inversion, and referencing to other tissue.

The results of our study indicate that CSvO₂ values were not found to be significantly different in injured preterm and term neonates compared with healthy term controls. One reason for this finding could be that preterm and term infants with moderate or severe HIE could have reduced CBF, which, along with a reduced oxygen metabolism, would result in CSvO₂ similar to that in healthy controls. In this case, injured neonates would have reduced oxygen metabolism and, thus, compromised brain health. To test these 2 opposing theories, however, we would require additional information, such as CBF and cerebral arterial oxygen saturation (CSaO₂). For instance, the oxygen extraction

fraction, the percentage of oxygen used from the blood as it passes through the capillary network, can be calculated by subtracting the fraction of oxygen saturation in the cerebral arteries (CSaO₂) from the fraction of oxygen saturation in the cerebral veins (CSvO₂).^{22,23} While CSaO₂ can be easily and noninvasively measured using a pulse oxygen monitor and CBF can be acquired using another MR imaging scan such as arterial spin-labeling or phase contrast,⁵⁵ our study, unfortunately, did not acquire these data because they were not part of the original study design. Thus, we cannot make more conclusive statements regarding preterm and term injured brain health. An alternative explanation could be because our data show premature rupture of fetal membranes in >60% of the preterm infants, which is higher than usual. It is possible that these infants have adapted to the outside world and have CSvO₂ values closer to term infants.

Two strengths of our method are as follows: The QSM algorithm is available for free on-line at <https://github.com/kamesy/QSM.m> for researchers and clinicians to download and use. Furthermore, our method of selecting venous susceptibility values (looking at the highest 0.25%) helps reduce human error using a completely data-driven process.

There are several limitations to the current study. Only 8 subjects from each group were examined, limiting our statistical power. We did not acquire CSaO₂ or CBF measurements, which would have allowed us to examine why both preterm and term infants with moderate or severe HIE did not show statistically significant differences in CSvO₂ compared with healthy controls. Furthermore, no follow-up with these patients was attempted, such as cognitive scores, which could have been used to investigate any correlations with CSvO₂. In the future, we hope to add more subjects, acquire CSaO₂ and CBF measurements (such as arterial spin-labeling), and perform cognitive measurements as the infants develop later in life. One piece of advice the authors wish to pass on to future researchers is the importance of acquiring and using Hct values in calculating CSvO₂. Had we used a constant value for Hct, the preterm group would have been found to have a statistically significant difference in CSvO₂. However, by using acquired Hct from each subject, this difference was no longer seen because Hct increases with gestational age and preterm infants were scanned at a younger gestational age.⁵⁶

CONCLUSIONS

We were able to measure CSvO₂ in the internal cerebral veins in healthy term, preterm, and term injured neonates. These values agree well with previously reported values in the literature. However, we did not see a difference in CSvO₂, despite the presence of HIE in the term injured and preterm infants. More studies should be performed in preterm and term infants with moderate or severe HIE, while acquiring other brain oxygen metrics such as CBF and CSaO₂ along with cognitive metrics as the infants develop later in life.

REFERENCES

1. Ferriero DM. Neonatal brain injury. *N Engl J Med* 2004;351:1985–95 [CrossRef Medline](#)
2. Kurinczuk JJ, White-Koning M, Badawi N. Epidemiology of neonatal encephalopathy and hypoxic-ischaemic encephalopathy. *Early Hum Dev* 2010;86:329–38 [CrossRef Medline](#)
3. Bryce J, Boschi-Pinto C, Shibuya K, et al. WHO estimates of the causes of death in children. *Lancet* 2005;365:1147–52 [CrossRef Medline](#)
4. Barkovich AJ, Hajnal BL, Vigneron D, et al. Prediction of neuromotor outcome in perinatal asphyxia: evaluation of MR scoring systems. *AJNR Am J Neuroradiol* 1998;19:143–49 [Medline](#)
5. Sarnat HB, Sarnat MS. Neonatal encephalopathy following fetal distress: a clinical and electroencephalographic study. *Arch Neurol* 1976;33:696–705 [CrossRef Medline](#)
6. Chalak LF, Rollins N, Morriss MC, et al. Perinatal acidosis and hypoxic-ischemic encephalopathy in preterm infants of 33 to 35 weeks' gestation. *J Pediatr* 2012;160:388–94 [CrossRef Medline](#)
7. Logitharajah P, Rutherford MA, Cowan FM. Hypoxic-ischemic encephalopathy in preterm infants: antecedent factors, brain imaging, and outcome. *Pediatr Res* 2009;66:222–29 [CrossRef Medline](#)
8. Laptook AR. Birth asphyxia and hypoxic-ischemic brain injury in the preterm infant. *Clin Perinatol* 2016;43:529–45 [CrossRef Medline](#)
9. Salhab WA, Perlman JM. Severe fetal acidemia and subsequent neonatal encephalopathy in the larger premature infant. *Pediatr Neurol* 2005;32:25–29 [CrossRef Medline](#)
10. Rana L, Sood D, Chauhan R, et al. MR imaging of hypoxic ischemic encephalopathy: distribution patterns and ADC value correlations. *Eur J Radiol Open* 2018;5:215–20 [CrossRef Medline](#)
11. Azzopardi D, Edwards AD. Magnetic resonance biomarkers of neuroprotective effects in infants with hypoxic ischemic encephalopathy. *Semin Fetal Neonatal Med* 2010;15:261–69 [CrossRef Medline](#)
12. Thayyil S, Chandrasekaran M, Taylor A, et al. Cerebral magnetic resonance biomarkers in neonatal encephalopathy: a meta-analysis. *Pediatrics* 2010;125:e382–395 [CrossRef Medline](#)
13. Skappak C, Regush S, Cheung P-Y, et al. Identifying hypoxia in a newborn piglet model using urinary NMR metabolomic profiling. *PLoS ONE* 2013;8:e65035 [CrossRef Medline](#)
14. Cainelli E, Trevisanuto D, Cavallin F, et al. Evoked potentials predict psychomotor development in neonates with normal MRI after hypothermia for hypoxic-ischemic encephalopathy. *Clin Neurophysiol* 2018;129:1300–06 [CrossRef Medline](#)
15. Pryds O, Greisen G, Lou H, et al. Vasoparalysis associated with brain damage in asphyxiated term infants. *J Pediatr* 1990;117:119–25 [CrossRef Medline](#)
16. Lassen NA. The luxury-perfusion syndrome and its possible relation to acute metabolic acidosis localised within the brain. *Lancet* 1966;2:1113–15 [CrossRef Medline](#)
17. Skov L, Pryds O, Greisen G, et al. Estimation of cerebral venous saturation in newborn infants by near infrared spectroscopy. *Pediatr Res* 1993;33:52–55 [CrossRef Medline](#)
18. Rescoe E, Tang X, Perry DA, et al. Cerebral near-infrared spectroscopy insensitively detects low cerebral venous oxygen saturations after stage 1 palliation. *J Thorac Cardiovasc Surg* 2017;154:1056–62 [CrossRef Medline](#)
19. Shmueli K, de Zwart JA, van Gelderen P, et al. Magnetic susceptibility mapping of brain tissue in vivo using MRI phase data. *Magn Reson Med* 2009;62:1510–22 [CrossRef Medline](#)
20. Deistung A, Schweser F, Reichenbach JR. Overview of quantitative susceptibility mapping. *NMR Biomed* 2017;30:e3569 [CrossRef Medline](#)
21. Haacke EM, Xu Y, Cheng Y-CN, et al. Susceptibility-weighted imaging (SWI). *Magn Reson Med* 2004;52:612–18 [CrossRef Medline](#)
22. Haacke EM, Tang J, Neelavalli J, et al. Susceptibility mapping as a means to visualize veins and quantify oxygen saturation. *J Magn Reson Imaging* 2010;32:663–76 [CrossRef Medline](#)
23. Tang J, Liu S, Neelavalli J, et al. Improving susceptibility mapping using a threshold-based K-space/image domain iterative reconstruction approach. *Magn Reson Med* 2013;69:1396–1407 [CrossRef Medline](#)
24. Doshi H, Wiseman N, Liu J, et al. Cerebral hemodynamic changes of mild traumatic brain injury at the acute stage. *PLoS One* 2015;10:e0118061 [CrossRef Medline](#)

25. Chai C, Guo R, Zuo C, et al. **Decreased susceptibility of major veins in mild traumatic brain injury is correlated with post-concussive symptoms: a quantitative susceptibility mapping study.** *Neuroimage Clin* 2017;15:625–32 [CrossRef Medline](#)
26. Chai C, Wang H, Chu Z, et al. **Reduced regional cerebral venous oxygen saturation is a risk factor for the cognitive impairment in hemodialysis patients: a quantitative susceptibility mapping study.** *Brain Imaging Behav* 2020;14:1339–49 [CrossRef Medline](#)
27. Antonucci R, Porcella A, Pilloni MD. **Perinatal asphyxia in the term newborn.** *Journal of Pediatric and Neonatal Individualized Medicine* 2014;3:e030269 [CrossRef](#)
28. Gopagondanahalli KR, Li J, Fahey MC, et al. **Preterm hypoxic-ischemic encephalopathy.** *Front Pediatr* 2016;4:114 [CrossRef Medline](#)
29. Sie LT, van der Knaap MS, Oosting J, et al. **MR patterns of hypoxic-ischemic brain damage after prenatal, perinatal or postnatal asphyxia.** *Neuropediatrics* 2000;31:128–36 [CrossRef Medline](#)
30. Barkovich AJ, Sargent SK. **Profound asphyxia in the premature infant: imaging findings.** *AJNR Am J Neuroradiol* 1995;16:1837–46 [Medline](#)
31. Denk C, Rauscher A. **Susceptibility weighted imaging with multiple echoes.** *J Magn Reson Imaging* 2010;31:185–91 [CrossRef Medline](#)
32. Schofield MA, Zhu Y. **Fast phase unwrapping algorithm for interferometric applications.** *Opt Lett* 2003;28:1194–96 [CrossRef Medline](#)
33. Li W, Wu B, Liu C. **Quantitative susceptibility mapping of human brain reflects spatial variation in tissue composition.** *Neuroimage* 2011;55:1645–56 [CrossRef Medline](#)
34. Kames C, Wiggermann V, Rauscher A. **Rapid two-step dipole inversion for susceptibility mapping with sparsity priors.** *Neuroimage* 2018;167:276–83 [CrossRef Medline](#)
35. Leenders KL, Perani D, Lammertsma AA, et al. **Cerebral blood flow, blood volume and oxygen utilization normal values and effect of age.** *Brain* 1990;113:27–47 [CrossRef Medline](#)
36. Doucette J, Wei L, Hernández-Torres E, et al. **Rapid solution of the Bloch-Torrey equation in anisotropic tissue: application to dynamic susceptibility contrast MRI of cerebral white matter.** *Neuroimage* 2019;185:198–207 [CrossRef Medline](#)
37. Sedlacik J, Rauscher A, Reichenbach JR. **Obtaining blood oxygenation levels from MR signal behavior in the presence of single venous vessels.** *Magn Reson Med* 2007;58:1035–44 [CrossRef Medline](#)
38. Portnoy S, Milligan N, Seed M, et al. **Human umbilical cord blood relaxation times and susceptibility at 3 T: human umbilical cord blood relaxation times and susceptibility at 3 T.** *Magn Reson Med* 2018;79:3194–3206 [CrossRef Medline](#)
39. Ferrari M, Mottola L, Quaresima V. **Principles, techniques, and limitations of near infrared spectroscopy.** *Can J Appl Physiol* 2004;29:463–87 [CrossRef Medline](#)
40. Davies DJ, Su Z, Clancy MT, et al. **Near-infrared spectroscopy in the monitoring of adult traumatic brain injury: a review.** *J Neurotrauma* 2015;32:933–41 [CrossRef Medline](#)
41. Murkin JM, Arango M. **Near-infrared spectroscopy as an index of brain and tissue oxygenation.** *Br J Anaes* 2009;103(Suppl 1):i3–13 [CrossRef Medline](#)
42. Fan AP, Bilgic B, Gagnon L, et al. **Quantitative oxygenation venography from MRI phase.** *Magn Reson Med* 2014;72:149–59 [CrossRef Medline](#)
43. Liu S, Buch S, Chen Y, et al. **Susceptibility-weighted imaging: current status and future directions.** *NMR Biomed* 2017;30:10.1002/nbm.3552 [CrossRef Medline](#)
44. Yadav BK, Buch S, Krishnamurthy U, et al. **Quantitative susceptibility mapping in the human fetus to measure blood oxygenation in the superior sagittal sinus.** *Eur Radiol* 2019;29:2017–26 [CrossRef Medline](#)
45. Jain V, Buckley EM, Licht DJ, et al. **Cerebral oxygen metabolism in neonates with congenital heart disease quantified by MRI and optics.** *J Cereb Blood Flow Metab* 2014;34:380–88 [CrossRef Medline](#)
46. Yadav BK, Krishnamurthy U, Buch S, et al. **Imaging putative foetal cerebral blood oxygenation using susceptibility weighted imaging (SWI).** *Eur Radiol* 2018;28:1884–90 [CrossRef Medline](#)
47. Neelavalli J, Jella PK, Krishnamurthy U, et al. **Measuring venous blood oxygenation in fetal brain using susceptibility-weighted imaging.** *J Magn Reson Imaging* 2014;39:998–1006 [CrossRef Medline](#)
48. Shetty AN, Lucke AM, Liu P, et al. **Cerebral oxygen metabolism during and after therapeutic hypothermia in neonatal hypoxic-ischemic encephalopathy: a feasibility study using magnetic resonance imaging.** *Pediatr Radiol* 2019;49:224–33 [CrossRef Medline](#)
49. Liu P, Huang H, Rollins N, et al. **Quantitative assessment of global cerebral metabolic rate of oxygen (CMRO₂) in neonates using MRI.** *NMR Biomed* 2014;27:332–40 [CrossRef Medline](#)
50. Wang Y, Spincemaille P, Liu Z, et al. **Clinical quantitative susceptibility mapping (QSM): biometal imaging and its emerging roles in patient care.** *J Magn Reson Imaging* 2017;46:951–71 [CrossRef Medline](#)
51. Zhang Y, Rauscher A, Kames C, et al. **Quantitative analysis of punctate white matter lesions in neonates using quantitative susceptibility mapping and R2* relaxation.** *AJNR Am J Neuroradiol* 2019;40:1221–26 [CrossRef Medline](#)
52. Bosemani T, Poretti A, Huisman TA. **Susceptibility-weighted imaging in pediatric neuroimaging.** *J Magn Reson Imaging* 2014;40:530–44 [CrossRef Medline](#)
53. Tortora D, Severino M, Malova M, et al. **Variability of cerebral deep venous system in preterm and term neonates evaluated on MR SWI venography.** *AJNR Am J Neuroradiol* 2016;37:2144–49 [CrossRef Medline](#)
54. Albayram MS, Smith G, Tufan F, et al. **Frequency, extent, and correlates of superficial siderosis and ependymal siderosis in premature infants with germinal matrix hemorrhage: an SWI study.** *AJNR Am J Neuroradiol* 2020;41:331–37 [CrossRef Medline](#)
55. Dolui S, Wang Z, Wang DJ, et al. **Comparison of non-invasive MRI measurements of cerebral blood flow in a large multisite cohort.** *J Cereb Blood Flow Metab* 2016;36:1244–56 [CrossRef Medline](#)
56. Jopling J, Henry E, Wiedmeier SE, et al. **Reference ranges for hematocrit and blood hemoglobin concentration during the neonatal period: data from a multihospital health care system.** *Pediatrics* 2009;123:e333–37 [CrossRef Medline](#)
57. van der Hoeven MA, Maertzdorf WJ, Blanco CE. **Continuous central venous oxygen saturation (ScvO₂) measurement using a fiber optic catheter in newborn infants.** *Arch Dis Child Fetal Neonatal Ed* 1996;74:F177–81 [CrossRef Medline](#)
58. Buchvald FF, Kesje K, Greisen G. **Measurement of cerebral oxyhaemoglobin saturation and jugular blood flow in term healthy newborn infants by near-infrared spectroscopy and jugular venous occlusion.** *Biol Neonate* 1999;75:97–103 [CrossRef Medline](#)
59. Wintermark P, Hansen A, Warfield SK, et al. **Near-infrared spectroscopy versus magnetic resonance imaging to study brain perfusion in newborns with hypoxic-ischemic encephalopathy treated with hypothermia.** *Neuroimage* 2014;85:287–93 [CrossRef Medline](#)
60. De Vis JB, Petersen ET, Alderliesten T, et al. **Non-invasive MRI measurements of venous oxygenation, oxygen extraction fraction and oxygen consumption in neonates.** *Neuroimage* 2014;95:185–92 [CrossRef Medline](#)